ISSN 0974 - 9373

Vol. 24 No. 1 (2020) **Journal of International Academy of Physical Sciences** pp. 69- 82

Dielectric and Electrical Characterization of Nd Modified BST Ceramic

B. B. Mohanty

Department of Physics
Betnoti College Betnoti, Mayurbhanj, Odisha, India

P. S. Sahoo, S Behera and L. K. Mishra

Department of physics
North Orissa Unuversity, Baripada,Mayurbhanj, Odisha India
Email: ps_rilly@yahoo.com

J. Panda

Department of Physics, B. I. E. T, Bhadrak. Odisha, India

R. N. P. Choudhary

Department of Physics, ITER, Bhubaneswar, Odisha, India

(Received December 30, 2019)

Abstract: Ba4SrNdTi3V7O30 is a tungsten bronze structured polycr y stalline ceramic sample synthesized following solid-state reaction route at high temperature (i.e., at 950 °C). The room temperature X- ray diffraction study reveals the formation of single-phase orthorhombic structure. Detailed investigation of dielectric properties of Ba4SrNdTi3V7O30 in a broad frequency range (102-106Hz) at various temperatures (330-5000C) strongly suggests that these properties of the material are both frequency and temperature dependent. The existence of a dielectric anomaly proposes the compound has a transition at ~ 424^{o}C temperature for all the frequencies .From the study of temperature dependence ac conductivity the values of activation energy obtained in different regions, suggest the mixed type conduction process (i.e., ionic–polaronic and space charge generated from the oxygen ion vacancies) in the material. The ac conductivity spectrum obeys Jonscher's universal power law.

Keywords: Ceramics, Electrical properties, dielectrics

1. Introduction

Researchers are very closely related to materials, their properties and devices. For over more than a decade research and review of different works of the scientists put a revolutionary development in designing various devices for application. Looking to the recent development in the field of materials study a polycrystalline sample Ba4SrNdTi3V7O30 belonging to tungsten bronze (TB) structure is prepared by solid state reaction route. The study of electrical properties like dielectric, impedance and conductivity of many ferroelectric compounds belonging to TB structure unfold wide application especially in ferroelectric devices such as transducers, actuators, capacitors, and ferroelectric memories by virtue of their attractive ferroelectric, pyroelectric, piezoelectric, and nonlinear optical properties[1–5].

The TB structure is a complex arrangement of distorted BO6 octahedra sharing corners in such a way that three different types of interstices (A, B and C) are available for cation occupying in the general formula (A1)2(A2)4(C)4(B1)2(B2)8O30. Generally, the smallest interstice C is empty, so the general formula is A6B10O30 for the filled tungsten–bronze structure. In this paper we focus on the dielectric and electrical properties of the lead free TB ferroelectric compound Ba4SrNdTi3V7O30 .

2. Experimental

2.1 Material preparation: The preparation of Ba4SrNdTi3V7O30 (BSNTV) polycrystalline sample is done using high purity (>99.9%) raw materials; BaCO3, SrCO3, Nd2O3, TiO2, V2O5 (M/S Sarabhai M. Chemicals, India), following a high-temperature mixed oxide process. Thorough mixing and grinding of these ingredients (taken in suitable stoichiometry), are done in dry and wet (methanol) medium for 2h each in an agate mortar. The powders obtained are then calcined at an optimized temperature (950 °C) and time (for 24 h) in air. Palletization of the calcined powder is done using uniaxial pressure of 5×106 N/m2. The pellets are then sintered in air at about 1000°C for 12 h to get the desired ceramic sample. Finally, the pellets are polished to make both the faces flat and parallel and then electroded with high purity air-drying silver paste and are dried at 150 0C before taking electrical measurements.

2.2. Material Characterization: The formation of compound is confirmed from the X-ray diffraction pattern of the presintered (calcined) powder by

X-ray diffraction (XRD) analysis using an X-ray powder diffractometer (Rigaku, Miniflex) at room temperature with CuKα radiation (λ=1.5405 Å) in a wide range of Bragg's angles 2θ (200≤ 2θ ≤800) at a scanning rate of 30/ minute. Microstructure of sintered pellet was recorded by JEOL JSM-5800 scanning electron microscope (SEM). The electrical impedance (Z), capacitance (C) and loss tangent have been measured as a function of frequency (100 Hz–1 MHz) at different temperatures (33–500 0C) with a computer-controlled impedance analyzer (PSM 1735, model: N4L).

3. Result and Discussion

3.1 Structural analysis: Figure 1 shows the room temperature XRD patterns of the sample. All peaks of the XRD pattern are indexed by using computer software package 'POWD MULT'[7]. The patterns display single phase orthorhombic TB structure.

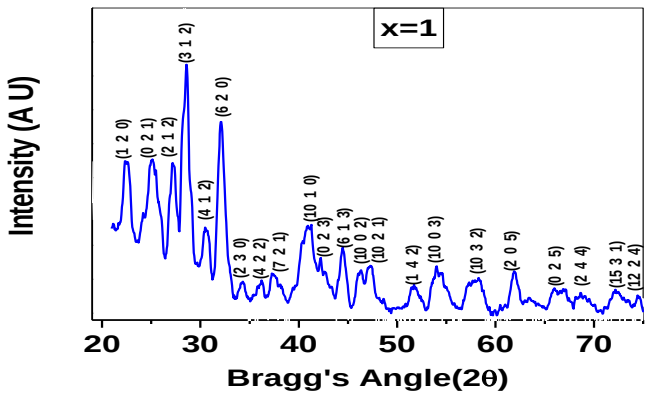

Figure 1. Room temperature XRD patterns of $Ba_4SrNdTi_3V_7O_{30}$

The best agreement between the observed (obs) and calculated (cal) inter planer spacing (d) (Σ (d_{obs} - d_{cal}) = minimum) of the compound is found in this system at room temperature. The least-squares refined unit cell parameters of the ceramics refined by the least-square method are: a = 8.0614 (33) Å, b =*7.5556*(33) Å, c=*22*.9113(33) Å for BSNTV (with standard deviation in parenthesis). Using the refined lattice parameters, interplaner spacing d of each reflection of the compound was calculated and compared with its observed value. The crystallite/particle size of the sample was estimated from the broadening of the XRD peaks ($\beta_{1/2}$), using

Scherrer's equation[8]; $P = K\lambda / \beta_{1/2}Cos\theta_{hkl}$, where K = constant = 0.89 and λ = 1.5405 Å. The average crystallite size of the compound is found to be 9.21 nm. The broadening of reflections due to mechanical strain and other effects has been ignored. The cell parameters are consistent and comparable to some of the compounds of this family [9,10].

3.2 Microstructural analysis: Figure 2 shows the scanning electron micro-g raph of the compound at room temperature describing its microstructure and surface property. The micrograph suggests the existence of polycrystalline texture of the sample as observed in XRD and having porous microstructure with the polycrystalline grains of typical dimensions in the range of 0.098μm. The distribution of grain is more or less homogeneous throughout the surface, but of non-uniform shape. Some of them are spherical in shape. Microstructure of this compound is comparable with that of other materials of this family[11].

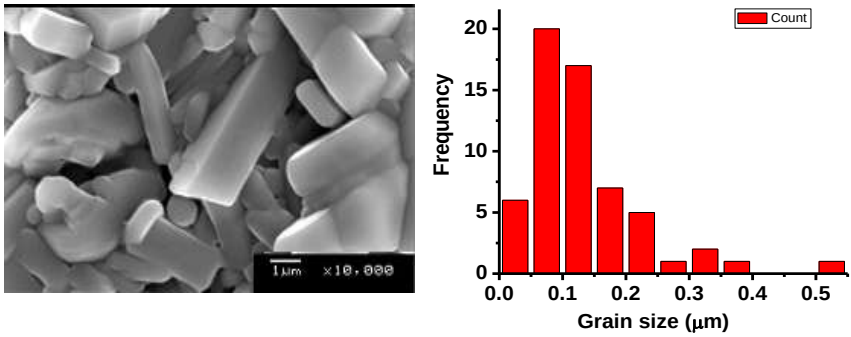

Figure 2. SEM micrographs and histogram (right) of $Ba_4SrNdTi_3V_7O_{30}$

3.3 Dielectric analysis: Figure 3 shows temperature dependence of relative dielectric constant (ε_r) of BSNTV at some selected frequencies.

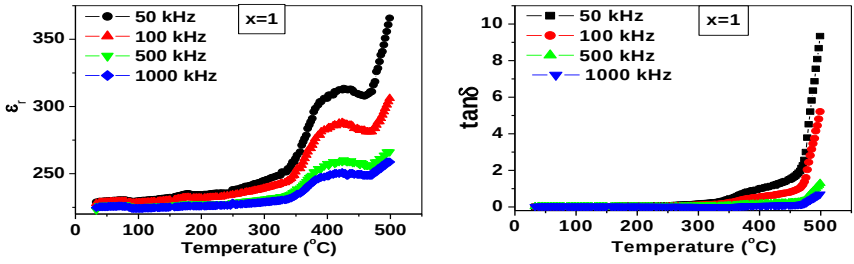

Figure 3. Variation of ε_r (left) and tanδ (right) with temperature of $Ba_4SrNdTi_3V_7O_{30}$ at some selected frequencies.

A single anomaly appears at 424^{o} C for all frequencies showing ferroelectric–paraelectric phase transition at this temperature. The dielectri constant of the sample at phase transition is found to be 314, 286, 256 and 249 at frequencies 50kHz, 100 kHz,500kHz and 1000kHz respectively. The frequency independent phase transition confirms that the compound is a non relaxor type of ferroelectric. From tan δ versus temperature plot (Figure 2 right), The value of loss tangent is almost zero upto 300^{o}C and thereafter it increases rapidly. The loss is very small below $T_{c,}$ and a change in slope observed at higher temperature.

3.4 Polarization study: The room temperature plot of polarization ~ electric field on poled sample is as shown in Figure 4. Presence of loop confirms the phase transition from ferro–paraelectric phase. The remnant polarization is measured to be $2P_r = 0.069\mu C/cm^2$ with externally applied electric field of strength 2.2485 kV/cm respectively

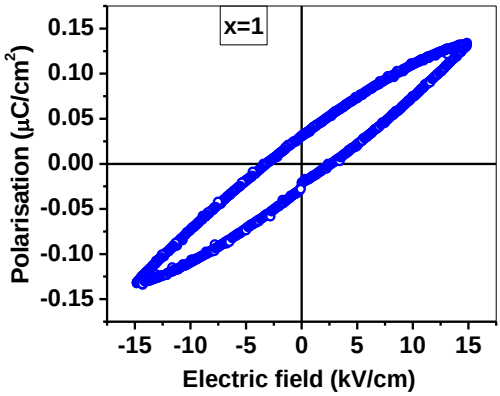

Figure 4. Room temperature hysteresis loop of $Ba_4SrNdTi_3V_7O_{30}$

3.5 ac conductivity study: The frequency dependence ac conductivity spectra of $Ba_4SrNdTi_3V_7O_{30}$ at some selected temperatures are shown in Figure 5. The ac conductivity spectra(σ_{ac}) is independent of frequency for entire frequency range and are also dispersive in nature for all the temperature which is due to electrode polarization. The flat plots are due to transition from long range hopping to short range ion motion and conductivity relaxation phenomenon[12]. The ac conductivity spectrum obeys Jonscher's universal power law.

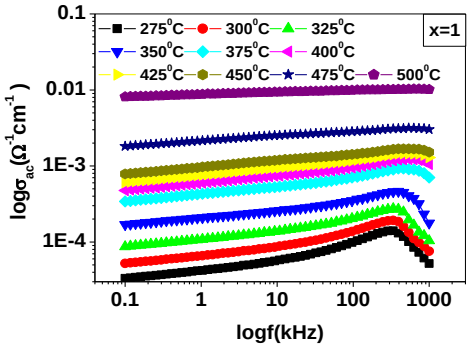

Figure 5. log σ_{ac} ~ log f of $Ba_4SrNdTi_3V_7O_{30}$ at some selected temperatures

The plot of σ_{ac} ~ absolute temperature (10^3/T) at different frequencies are shown in Figure 6. In low-temperature region, σ_{ac} is highly frequency dependent but is nearly independent of temperature. Such frequency dependence of σ_{ac} has been attributed to a wide distribution of relaxation time due to spread in jump distances[13]. The plots are linear over a wide temperature region obeying the Arrhenius relation.

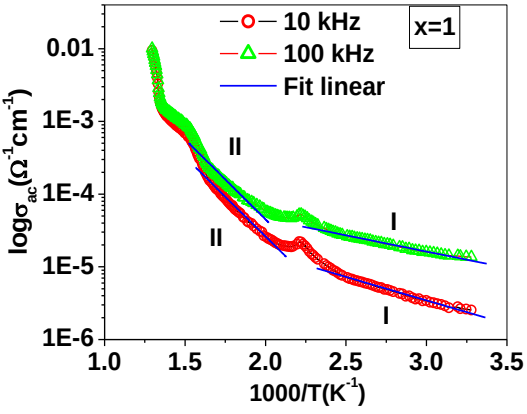

Figure 6. Variation of σ_{ac} with 1000/T of $Ba_4SrNdTi_3V_7O_{30}$ at two selected frequencies

Negative temperature coefficient of resistance (NTCR) type behavior in the material is noticed from conductivity study as is observed in semiconductors. An anomaly is observed at dielectric phase transition

temperature (i. e. at 424^{o}C). The two curves merged at high temperature exhibiting frequency independent dc conduction phenomena confirming the conductivity mechanism in the material is due to the onset of intrinsic type of charge carriers[14]. The value of activation energy (E_a) in different regions calculated from slope of Arrhenius plot (σ_{ac} ~ inverse of temperature) in various zones are given in the table.

Table 1. Comparison of activation energy Ea (eV) of $Ba_4SrNdTi_3V_7O_{30}$ at two different frequencies in region I, II calculated from σ_{ac} vs. 1/T graphs

Frequency in kHz	**Region I**	**Region II**
10	0.1283	0.4340
100	0.0887	0.4364

3.6 Impedance analysis: Complex impedance spectroscopy (CIS) is the most reliable technique to explain the electrical behavior of a system which include a number of strongly coupled processes. It makes easier to separate grain (intragrain) and grain boundaries (intergrain) contributions in transport properties of the material.

The temperature dependent Z' ~Z'' (complex impedance spectrum) of BSNTV measured at some selected temperatures (30–500^{0}C) is shown in Figure 7 for both high and low temperatures. At high temperature two merged semicircular arcs are observed in the spectrum suggesting the electrical response is both due to grain and grain boundary activities within the material. This response is equivalent to two parallel RC series connected in series as inserted in figure. The decrease in resistivity is confirmed from the shift in the point of interception of the arcs towards the origin of the complex plane plot on the real axis. This decrease in the resistive behavior of the sample is assisted by the grain boundary conduction with rise in temperature[15]. At low temperature single semicircular arc s are observed contributed by grain effect only.

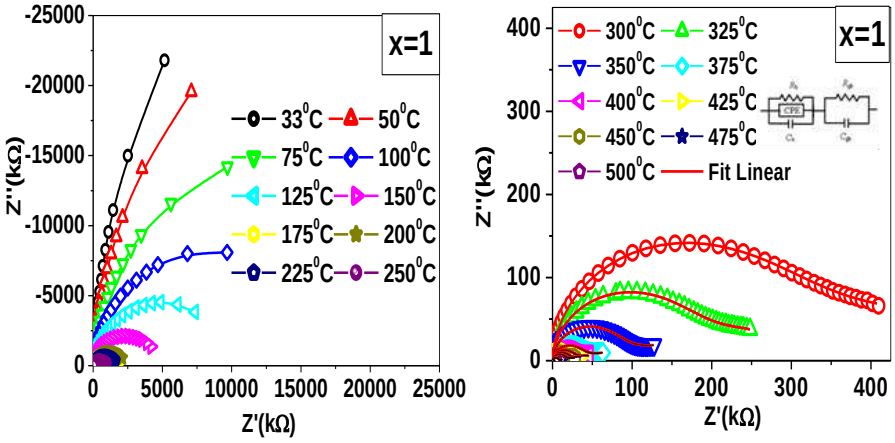

Figure 7. Nyquist plots of $Ba_4SrNdTi_3V_7O_{30}$ at different temperatures

The loss spectra or frequency dependent Z″ of Ba4SrNdTi3V7O30 at different temperatures is shown in Figure 8. Peaks are observed which shift towards higher frequency side with increasing temperature along with broadening of the peaks and decrease in peak height. Spreading of relaxation time is confirmed from the broadening of peaks suggesting the existence of temperature dependent electrical relaxation phenomenon in the compound[16]. This is due to thermally activated dielectric relaxation process and reduction of bulk resistance with temperature in the material. The merging of the dispersion curves at higher frequencies is because of liberation of space charges[17].

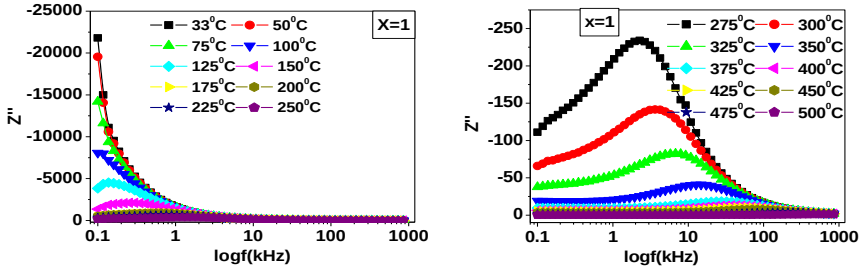

Figure 8. Loss spectra of $Ba_4SrNdTi_3V_7O_{30}$ at different temperatures

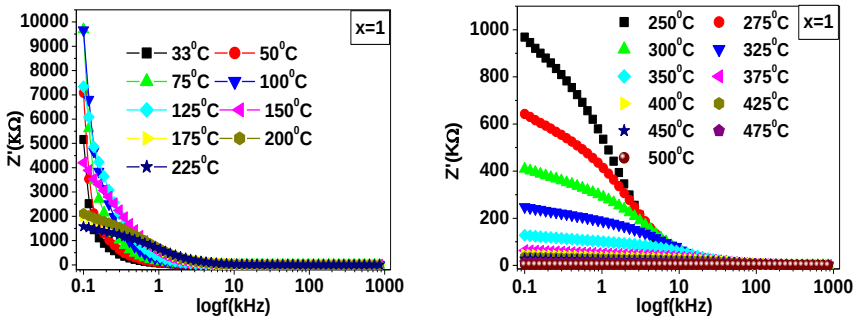

Figure 9. Z' ~ frequency graphs of $Ba_4SrNdTi_3V_7O_{30}$ (x =1) at different temperatures

The variation of Z' as a function of frequency (0.1–1000 kHz) at different temperatures (30–500^{0}C) is as shown in Figure 9. At low frequency the figure shows spike like response at almost all temperatures and also dispersion spreads in a high frequency regime with increase in temperature. The Z' value is found to be increasing with increase in temperature showing PTCR behavior up to a particular temperature (~150^{o}C)[18] in low temperature region and then decrease with increasing temperature showing NTCR behavior whereas in pure Ba based compound shows NTCR behavior in all temperature range, some other compounds also show similar types of behavior. The Z' value rises to a large extent both at low and high temperatures.

Extrapolation: Figure 10 shows the extrapolated plots of Z' vs. frequency and Z'' vs. frequency, using KK relation, for all the compounds at some selected temperature. Left side of solid line in the graph marks extrapolated data and right side of the line represents the measured data. The frequency range chosen for the extrapolation is two decades below the minimum measured frequency.

The validity of the measured data is checked by using a new algorithm[19]. The main objective of this algorithm is to find out the real and imaginary component of the complex impedance within a finite frequency limit, more specifically in the low frequency limit where the possibility of deviation is more. The validity of the measured data is check by the following algorithm

$$Z'(\omega) = \sum_{k=0}^{K} a_k^{(1)} (\log \omega)^k$$

$$Z''(\omega) = \sum_{m=0}^{M} a_m^{(2)} (\log \omega)^m$$

Where (c) is internally consistent with (d) and vice-versa. The polynomial orders, k and m are same as m. Also, the polynomial order is optimized by testing the data for different orders (i.e., 4-8 order). KK response is very much sensitive to errors (if present in the dataset). This can be observed as discontinuity in the real and imaginary part of the impedance. Measured data for the sample exhibits a good agreement with the extrapolated data.

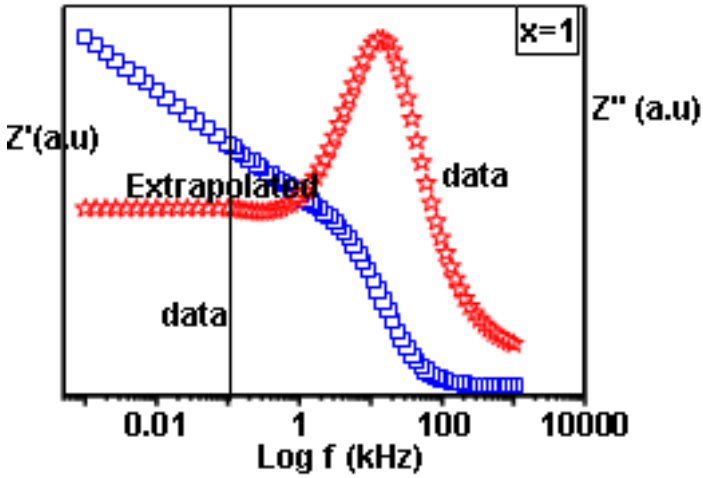

Figure 10. Z'~ log frequency and Z'' ~ log frequency, extrapolated using KKR of $Ba_4SrNdTi_3V_7O_{30}$ at some selected temperatures.

3.7 Complex modulus analysis: The complex modulus spectrums (M′ versus M″) of BSNTV at some selected temperatures are as shown in Figure 11.

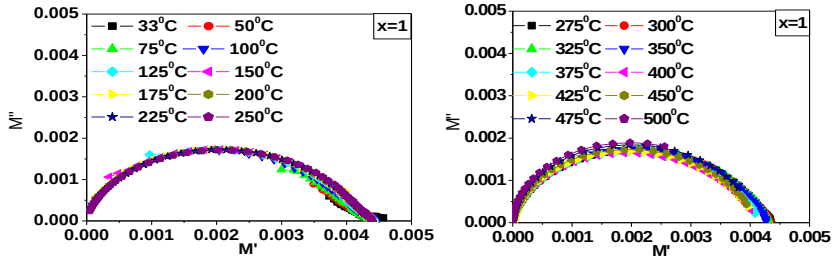

Figure 11. M″ versus M′ plots of $Ba_{5-x}Sr_xNdTi_3V_7O_{30}$ (x =0-2) at different temperature

The material exhibits electrical relaxation process, confirmed from the semicircular arc which appears to overlap at all the temperatures. The intercept on the real axis indicates the total capacitance contributed by the grain. The electrical properties of materials showing a single circular arc in complex modulus plane are defined by the parallel combination of grain capacitance (C) and resistance (R). In the compounds no exact semicircles are obtained. The formation of depressed semicircles with centers positioned below the x-axis indicates the spreading of relaxation time and hence non-Debye type of relaxation in these compounds. At low frequencies, the Nyquist plots of electric modulus exhibit the poly-dispersive nature for the dielectric relaxation. The appearance of asymmetric semicircular arcs indicates the electrical relaxation phenomenon in the materials.

The complex modulus loss spectra (frequency versus M″) of BSNTV at some selected temperatures are as shown in Figure 12. The figure exhibits well resolved asymmetric broadening in peak caused by (i) the random orientation of anisotropically conducting species, (ii) the presence of phases of more than one composition or structure[20] (iii) spread of relaxation times with different time constant due to local defects, which confirms a non-Debye type of relaxation.

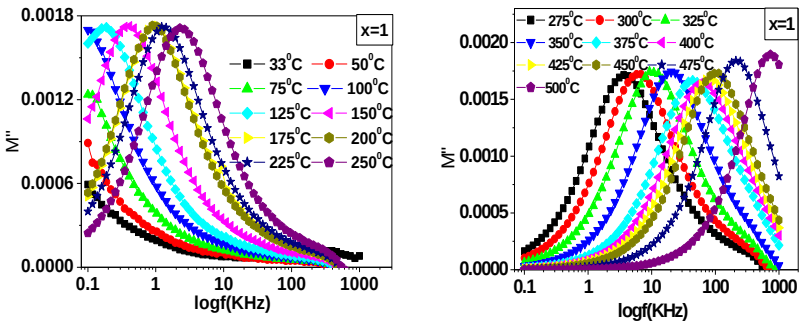

Figure 12. Frequency response of M" of $Ba_{5-x}Sr_xNdTi_3V_7O_{30}$ (x=1) at different temperatures

Shifting of peaks towards high frequency side with rise in temperature confirms the thermally activated non-Debye type of relaxation process in which hopping of charge carriers with small polarons is dominated intrinsically[21]. The presence of peak indicates long to short range mobility of charge carriers with increase in frequency. The frequency variation of real modulus (M') at different temperature is as shown in Figure 13.

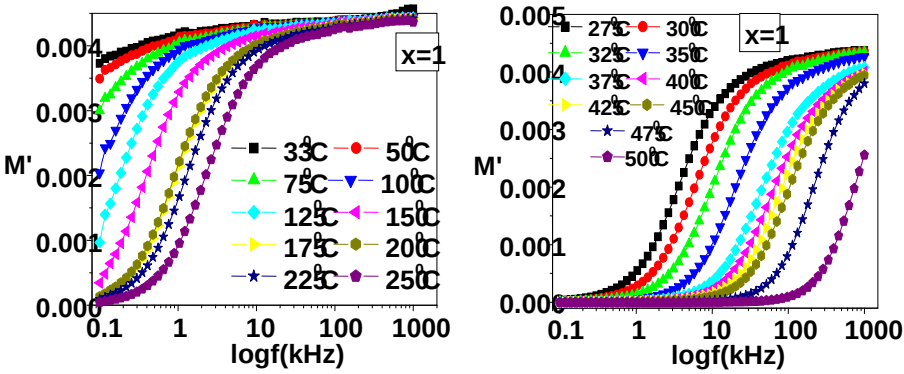

Figure 13. Frequency response of M' of $Ba_4SrNdTi_3V_7O_{30}$ at different temperatures

The low temperature plots approach to saturation at higher frequency side possessing maximum value of M' irrespective of temperature for all compounds. This is because of deficiency of restoring forces regulating the mobility of charge carriers in presence of an induced electric field[22]. But at high temperatures, at low frequencies, M' approaches to zero followed by a continuous dispersion with increase in frequency for all compounds. The saturation of M' at high frequency region is not seen in high temperature region.

4. Conclusions

The polycrystalline ceramic sample synthesized following solid-state reaction route at high temperature (i.e., at 950°C). The room temperature X-ray diffraction study reveals the formation of single-phase orthorhombic structure. From SEM study distribution of grain is more or less homogeneous throughout the surface, but of non-uniform shape. Anomaly appeared at 424°C for all frequencies showing ferroelectric–paraelectric phase transition at this temperature. Presence of hysteresis loop confirms the phase transition from ferro to paraelectric phase. The ac conductivity spectrum obeys Jonscher's universal power law. Negative temperature coefficient of resistance (NTCR) type behavior in the material from conductivity study as is observed in semiconductors. Two merged semicircular arcs are observed in the impedance spectrum suggesting the electrical response is both due to grain and grain boundary activities within the material. Z' decreases with rise in both temperature and frequency

indicates the existence of negative temperature coefficient of resistance (NTCR) type behavior in the material as is observed in semiconductors whereas, in low temperature PTCR behavior is observed up to a particular temperature (~150^{o}C).The complex modulus spectra show depressed semicircles with centers positioned below the x-axis indicating the spreading of relaxation time and hence non-Debye type of relaxation in these compounds. The extrapolation curve for Z' vs. frequency and Z'' vs. frequency for the sample exhibits a good agreement between the measured and extrapolated data.

References

1. B. Jaffe, W. R. Cook and H. Jaffe, *Piezoelectric Ceramics*, Academic Press, London, 1971.

2. K. Uchino, *Piezoelectric Actuators and Ultrasonic Motors*, Kluwer Academics, Boston, 1997.

3. R. R. Neurgaonkar, M. H. Kalisher, T. C. Lim, E. J. Staples and K. L. Keester, Czochralski Single Crystal Growth of Sr.61Ba.39Nb2O6 for Surface Acoustic Wave Applications, *Materials Research Bulletin*, **15(9)** (1980), 1235-1240

4. W. Sakamoto, Y. Horie, T. Yogo and S. Hirano, Synthesis and Properties of Highly Oriented (Sr, Ba)(Nb, Ta)2O6 Thin Films by Chemical Solution Deposition , Jpn. J. Appl. Phys, **40** (2001), 5599-5604.

5. P. Ganguly, A. K. Jha, Investigations Of Dielectric, Pyroelectric and Electrical Properties of Ba5SmTi3Nb7O30 Ferroelectric Ceramic, *Journal of Alloys and Compounds*, **484 (1-2)**, (2009), 40-44.

7. Powdmult, *An interactive powder diffraction data interpretations and indexing Program Version 2.1*, E. WU School of Physical Sciences, Flinder University of South Australia Bradford Park, SA 5042, Australia.

8. P. Scherrer, G. Nachrichten, Bestimmung der inneren Struktur und der Größe von Kolloidteilchen mittels Röntgenstrahlen, *Kolloidchemie Ein Lehrbuch*, **2** (1918), 98-100.

9. M. R. Ranga Raju and R. N. P. Choudhary, Structural, Dielectric and Electrical Properties of Sr5RTi3Nb7O30 (R=Gd And Dy), *Ceramics Material Letters*, **57** (2003), 2980-2987.

10. B. Behera, P. Nayak and R. N. P. Choudhary, Structural, Dielectric and Electrical Properties of Naba2x5o15 (X = Nb And Ta), *Ceramics Mater. Lett.*, **59** (2005), 3489-3493.

11. B. Behera, P. Nayak and R. N. P. Choudhary, Structural, Dielectric and Electrical Properties of Liba2x5o15 (X = Nb And Ta), *ceramics, Mater. Chem. Phys*., **100** (2006), 138-141.

12. R. Mizaras, M. Takashige, J. Banys, S. Kojima, J. Grigas, Hamazaki, Sin- Ichi and A. Brilingas, Dielectric Relaxation in Ba 2NaNb 5(1- x)Ta 5 xO 15 Single Crystrals, *J. Phys. Soc. Jpn.*, **66** (1997), 2881-2885

13. M. Pollock and T. H. Geable, Low-Frequency Conductivity Due to Hopping Processes in Silicon, *Phys. Rev.*, **122** (1961), 1742.

14. O. Raymond, R. Font, N. Suárez-Almodovar, J. Portelles and J. M. Siqueiros, Frequency- Temperature Response of Ferroelectromagnetic Pb(Fe1⁄2Nb1⁄2)O3 Ceramics Obtained by Different Precursors. Part II. Impedance Spectroscopy Characterization, *J. Appl. Phy.*, **97** (2005), 084107-114.

15. A. K. Jonscher,*The Universal Dielectric Response, Nature*, **267** (1977), 673-679.

16. N. Zidi, A. Chaouchi, S. dAstorg, M. Rguiti and C. Courtois, Dielectric and Impedance Spectroscopy Characterizations of Cuo Added $(Na_{0.5}Bi_{0.5})_{0.94}Ba_{0.06}tio_3$ Lead-Free Piezoelectric Ceramics, *J. Alloys and Comp.*, **590** (2014), 557-564.

17. K. S. Rao, D. M. Prasad, P. M. Krishnal and J. H. Lee, Frequency Dependent Electrical Characteristics of Ferroelectric $Pb_{4.0}K_{1.0}Li_{1.0}Nb_{10}O_{30}$ Ceramics, *Eur. Phys. J. Appl. Phys.*, **39** (2008), 237-249.

18. A. R West, D. C Sinclair and Naohiro Hirose, Characterization of Electrical Materials, Especially Ferroelectrics by Impedance Spectroscopy, *J. Elect. Ceramics*, **1(1)** (1997), 65-71.

19. J. M. Esteban and M. E. Orazem, On the Application of the Kramers-Kronig Relations to Evaluate the Consistency of Electrochemical Impedance Data, *J. Electrochemical Society*, **138(1)** (1991), 67-76.

20. M. Hodge, M. D. Ingram and A. R. West, A New Method for Analysing the A. C. Behaviour of Polycrystalline Solid Electrolytes, *Electrochemistry*, **58** (1975), 429-432.

21. B. Behera, P. Nayak and R. N. P. Choudhary, Structural, Dielectric and Electrical Properties of Liba2x5o15 (X= Nb And Ta) Ceramics, *Mater. Chem. Phys.*, **100 (1)** (2006), 138-141.

22. P. B. Macedo, C. T. Moynihan and R. Bose, The Role of Ionic Diffusion in Polarization in Vitreous Ionic Conductors, *Phys. and chem. of Glasses*, **13** (1972), 171-179.